In: Kruhl JH (Ed.)
Fractals and Dynamic Systems in Geoscience.
Springer, Berlin, 1994.

Fractal Analyses of Pleistocene Marine Oxygen Isotope Records

Michael Schulz[1], Manfred Mudelsee[2] & Thomas C.W. Wolf-Welling[1]
[1]GEOMAR, Forschungszentrum für marine Geowissenschaften,
Wischhofstr. 1-3, D-24148 Kiel, Germany
[2]Geologisch-Paläontologisches Institut, Universität Kiel,
Olshausenstr. 40, D-24118 Kiel, Germany

Abstract. Fractal dimensions of oxygen isotope ($\delta^{18}O$) data obtained from deep-sea records were estimated. The globally distributed data reflect climate variability during the late Pleistocene.

All fractal dimensions fall into the range of $1 < D < 2$. However, the records do not show self-affinity over the entire range of investigated time scales, instead two significantly different fractal dimensions can be observed. This result contrasts with previous suggestions that time series obtained from climate proxies might possess self-affinity with a single fractal dimension over a range of 10 to 10^5 years.

The estimated fractal dimensions of the $\delta^{18}O$ records for time scales between 3 and ~20 ka fall into a narrow range, with an average value of $D = 1.51 \pm 0.06$.

Estimated fractal dimensions for longer time scales may be biased by the presence of periodic components in the time series. The limited range of time scales which can be described by a *single* fractal dimension raises questions about the applicability of simple fractal theory to this kind of data.

Introduction

A very common characteristic of many natural phenomena is their scale invariance, that is, an object looks the same under a change of resolution. Typical examples include the shape of clouds and rock surfaces. Mandelbrot (1967) introduced the term fractal to describe this scale invariance. A fractal can be described as an object made of parts similar to the whole in some way, i.e. in a statistical sense (Feder 1988). A statistically self-similar fractal in a two-dimensional (x,y) space can be defined as follows (Turcotte 1992, p 74): $f(x,y)$ is statistically similar to $f(rx,ry)$, where r is a scaling factor. In this case both variables are scaled by the same scaling-factor.

When dealing with time series similarity transformations usually require different scaling factors for time axis and the variable being measured as a function of time. A time series can be described as a self-affine fractal if $f(t,y)$ is statistically similar to $f(rt,r^H y)$, where r is again a scaling factor and H is the Hausdorff dimension. The latter is related to the fractal dimension D by:

$D = 2- H$ (Turcotte 1992, p 75). If D falls into the range of $1 < D < 2$ the time series is called a 'fractional Brownian function' (Mandelbrot 1977).

Here we investigate whether late Pleistocene time series of oxygen isotopes ($\delta^{18}O$) can be described as fractals. The $\delta^{18}O$ records reflect changes in continental ice volume and to a lesser degree variations in ocean water temperature, hence, they can be regarded as climate proxy data. The fractal approach is purely descriptive, therefore, no *direct* information about the underlying physical processes documented by the $\delta^{18}O$ data is obtained.

In addition, we address the question as to whether or not a global fractal dimension exists describing climatic fluctuations over the entire Pleistocene as previously suggested by Fluegeman and Snow (1989).

Method

To determine the fractal dimension of the various time series we follow a method developed by Higuchi (1988). Given an evenly spaced time series $Y_1, Y_2, \ldots, Y_N$, first new time series are constructed:

$$Y_k^m = Y_m, Y_{m+k}, Y_{m+2k}, \ldots, Y_{m+\left[\frac{N-m}{k}\right]\cdot k} \quad (m = 1, 2, \ldots, k),$$

where [...] denotes integer notation, m is the initial time and k the interval time, both being integers. For any time interval k, k new time series can be constructed. Now the *length* of each time series Y_k^m is given by:

$$L_m(k) = \left\{ \left(\sum_{i=1}^{\left[\frac{N-m}{k}\right]} \left| Y_{m+ik} - Y_{m+(i-1)\cdot k} \right| \right) \cdot \frac{N-1}{\left[\frac{N-m}{k}\right]\cdot k} \right\} \cdot \frac{1}{k} \qquad (1)$$

The length of the curve for a time interval k, $\langle L(k) \rangle$ is defined as the average over k sets of $L_m(k)$:

$$\langle L(k) \rangle = \frac{1}{k} \cdot \sum_{m=1}^{k} L_m(k) \qquad (2)$$

For a statistically self-affine curve in a (x,y)-plane

$$\langle L(k) \rangle \propto k^{-D}, \qquad (3)$$

where D is the fractal dimension. The interval time k is related to the time scale τ by: $\tau = \Delta t \cdot k$, where Δt denotes the time interval between the equidistant data points (e.g. 3 ka).

Compared to the spectral method (e.g. Turcotte 1992; p 74), the advantage of the Higuchi method is that relatively short time series will result in stable estimations of the fractal dimension (Higuchi 1988). In addition, a change of the fractal dimension over the investigated time range can be identified more easily.

Before determining the fractal dimensions of the $\delta^{18}O$ records, all time series were linearly interpolated to obtain equidistant time series. The interpolation was performed in such a manner that the number of points in the interpolated time series is equal to the number of original data points. Subsequently, a linear trend was subtracted from the data. Instead of fitting a linear function in log-log space to the calculated $[k,\langle L(k)\rangle]$ data we fitted the nonlinear model (Eq. 3) to the points, since any linearization of the data may lead to wrong results when using a least-square method for fitting a function to the transformed points (Appendix). Fitting the nonlinear model was carried out by numerical approximation using the Levenberg-Marquardt method (e.g. Press et al. 1989).

Fractal dimensions were calculated for all possible sets of $[k,\langle L(k)\rangle]$ with ≥ 3 data pairs. To evaluate the goodness-of-fit of the resulting models, the χ^2 probability for each fit was calculated. To do so, first the uncertainties associated with the determined $\langle L(k)\rangle$ must be evaluated. With the known errors of the measured parameters (section "Data Material") this was done by applying the laws of error propagation to Equations 1 and 2. The probability of a significant fit decreases with increasing number of $[k,\langle L(k)\rangle]$ points used for a certain fitting procedure. Hence, one would obtain the highest probabilities if the entire set of $[k,\langle L(k)\rangle]$ were divided into relatively short segments (e.g. 3 points per segment). This would result in a large number of fractal dimensions, each valid for a short time scale only. Since we are interested in describing the time series by as few fractal dimensions as possible, one has to find a compromise between the goodness-of-fit of the fitting function and the length of the segments for which the fractal dimension are estimated. Evaluation of the fitting results was guided by the following criteria:

- χ^2 'Goodness-of-fit' probability ≥ 0.1,
- interval-length $[\tau_{min}, \tau_{max}]$ comparable between the records.

Data Material

The $\delta^{18}O$ time series used for the fractal analyses were obtained from published Pleistocene deep-sea records and comprise the last 380-1000 ka with resolutions in the order of 2-5 ka (a typical $\delta^{18}O$ record is shown in Figure 1). Core locations and characteristics are summarized in Table 1. Depending on the depth of the core sites and the depth habitat (benthic vs. planktonic) of the foraminifera

Table 1. Summary of the core locations and characteristics. * denotes a modified stratigraphy based on (Shackleton et al. 1990); T_{cont}: continuous part of the record used for the present study; Δt: time interval of the linearly interpolated time series; N: number of data points; Foram: indicates whether $\delta^{18}O$ data were measured on *Planktonic* or *Benthic foraminifera*. Last column indicates the source of the data: 1. Nelson et al. 1986; 2. Ruddiman et al. 1989; 3. Wolf 1991; 4. Tiedemann 1991; 5. deMenocal et al. 1993; 6. Shackleton and Hall 1989; 7. Shackleton et al. 1990; 8. Mix et al. 1991; 9. Clemens et al. 1991.

Core	Latitude	Longitude	Depth [m]	T_{cont} [ka]	Δt [ka]	N	Foram	'Sampled' Ambient Water Mass	Ref.
DSDP 594*	45°31'S	174°75'E	1204	9-972	3.0	322	P	Sub-Antarctic Surface Water	1
DSDP 594*	45°31'S	174°75'E	1204	8-968	4.0	241	B	Antartic Intermediate Water	1
ODP 607*	41°00'N	32°58'W	3427	245-998	3.0	251	B	North-Atlantic Deep Water	2
ODP 643*	67°43'N	01°02'E	2780	4-501	3.5	143	P	Norwegian-Sea Water	3
ODP 658	20°45'N	18°35'W	2263	76-661	1.8	326	B	North-Atlantic Deep Water	4
ODP 663	01°12'N	11°53'W	3708	0-915	3.0	306	P	South-Atlantic Central Water	5
ODP 677	01°12'N	83°44'W	3461	5-993	2.6	381	B	Pacific Deep Water	6,7
RC 13-110	00°06'N	95°39'W	3231	3-735	3.0	245	B	Pacific Deep Water	8
RC 27-61	17°00'N	60°00'E	1893	6-432	3.0	143	P	Arabian-Sea Water	9
V 19-27	00°28'S	82°04'W	1373	2-376	2.0	188	B	Antarctic Intermediate Water	8

Fig. 1. Oxygen isotope record spanning the last 900 ka obtained from deep-sea core ODP 663 (deMenocal et al. 1993). The $\delta^{18}O$ time series mainly reflects changes in continental ice volume, with more negative values indicating less ice (Note that the ordinate scale is inverted).

used for the $\delta^{18}O$ determination, the data document the $\delta^{18}O$ variations of the ambient water masses of the core sites, i.e. upper, intermediate and deep water masses.

All $\delta^{18}O$ data are reported relative to the PDB standard. Random errors associated with the $\delta^{18}O$ determination arise from analytical uncertainties (0.05 to 0.07‰) and random variations in the sample population (e.g. habitat effects). Mix (1992) estimated the combined random error to be in the order of 0.1‰. This value was used for all data sets to evaluate the goodness-of-fit (above). The age models of all $\delta^{18}O$ records are based on oxygen isotope stratigraphy. Whenever a $\delta^{18}O$ record contains a hiatus only the continuous parts of the time series was used (Table 1). Although some of the time series document climatic variations throughout the entire Pleistocene and upper Pliocene, only those parts younger than 1 Ma were used for the present study, because there is evidence for a fundamental change in the mode of the climatic variations around this time (e.g. Ruddiman et al. 1986).

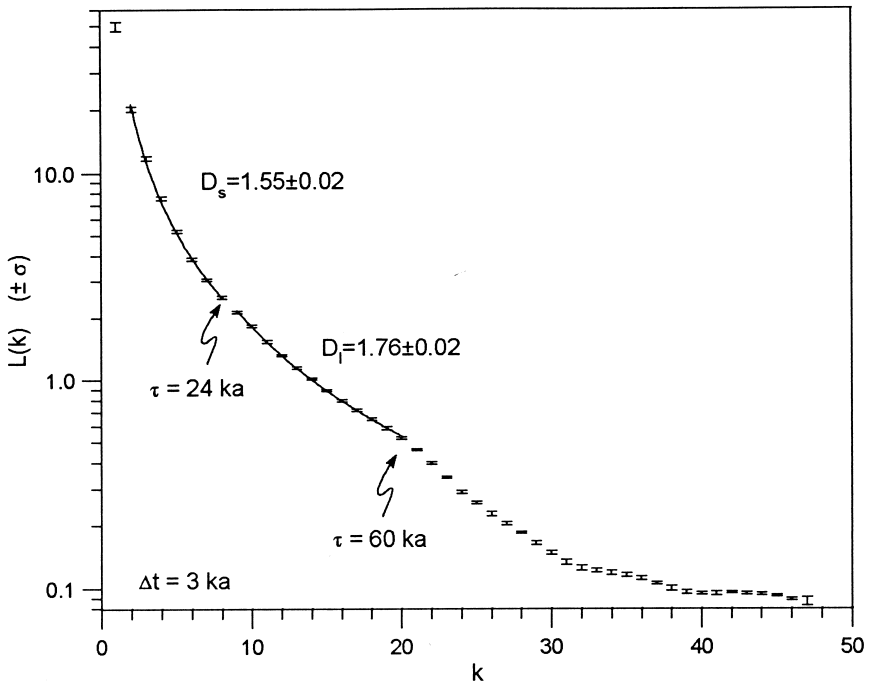

Fig. 2. Determination of the fractal dimensions for the $\delta^{18}O$ record of ODP 663. $\langle L(k)\rangle$ is the 'length' of the time series as a function of a 'time yardstick' k. The dimensions were obtained by fitting a nonlinear model to the $[k,\langle L(k)\rangle]$ points. The parameter k is related to the actual time scale, τ by $\tau = k \cdot \Delta t$, where Δt is the linearly interpolated sampling interval. Note that the fractal dimension describing the time series changes at $\tau = 24$ ka and that for $\tau > 60$ ka no significant fit is possible.

Results of the Fractal Analyses

Figure 2 shows a typical example of a $[k,\langle L(k)\rangle]$ plot and the fitted nonlinear function used to determine the fractal dimension. Figure 3 summarizes all fractal dimensions obtained from the time series which pass the above mentioned requirements. The estimated fractal dimensions cover an interval between $1.42 < D < 1.93$, hence all time series may be described as fractional Brownian functions.

However, it is also obvious from Figure 3 that the $\delta^{18}O$ records do not show a unique fractal dimension over the entire time scale ($k_{max} \cdot \Delta t$) being investigated. Instead, two significantly different fractal dimensions can be observed at each core (except data from core DSDP 594): a lower fractal dimension for short time scales ranging from ~3-20 ka (τ_s group) and a significantly higher dimension for longer time scales between ~20-60 ka (τ_l group). For time scales longer

than approximately 60 ka it becomes impossible to yield a significant fit of a model according to Equation 3.Considering the τ_s group the lowest fractal dimensions can be observed for two of the deep-water $\delta^{18}O$ records (ODP 658 and RC 13-110). An exceptionally high fractal dimension was determined for core ODP 643, falling into the range of the τ_l group. The average fractal dimension of this group (excluding the outlier from the poor resolution record ODP 643) is $D_s = 1.51 \pm 0.06$. (Mean values are given as weighted means and errors as weighted sample standard deviations throughout the text.)

The τ_l group is characterized by slightly more scattered fractal dimensions as compared to the τ_s group ($D_l = 1.79 \pm 0.08$). There seems to be no obvious relation between fractal dimensions and water masses. A comparison of the difference between the fractal dimensions, i.e. $D_{t_s} - D_{t_l}$ for each core, shows that the largest differences occur for deep-water $\delta^{18}O$ data.

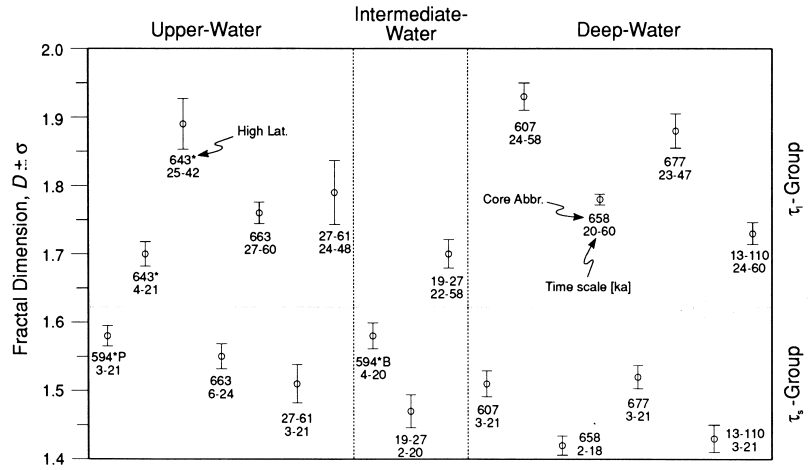

Fig. 3. Synopsis showing the fractal dimensions determined for the various $\delta^{18}O$ records. Cores have been sorted according to the type of ambient water mass (Table 1). Note that only the core numbers from Table 1 are used to identify the cores. High latitude cores are marked by '*'. Also shown is the time scale interval for which the fractal dimension was determined. Errors are reported as sample standard deviations. The horizontal line (dotted) separates the τ_s group from the τ_l group (see text for further explanations).

Discussion and Conclusions

The concept of fractals was introduced in order to describe scale *invariance*, i.e. the notion that $f(t,ry)$ is statistically similar to $f(rt,r^H y)$ even if the scaling factor r changes over several orders of magnitude. Considering the nature of the $\delta^{18}O$ data, one is confronted with the fact that the range of possible time scales

comprises less than two orders of magnitude (3 ka < τ < 150 ka). Moreover, since it is not possible to find fractal dimensions for the $\delta^{18}O$ records for time scales larger than 60 ka, the scale variation decreases to about one order of magnitude. This limitation raises questions concerning the applicability of simple fractal theory to this kind of data and should be kept in mind during the following discussion.

The finding that the $\delta^{18}O$ records cannot be adequately described by a single fractal dimension over the entire range of investigated time scales contrasts with previous suggestions that time series obtained from climate proxies might possess self-affinity with a single fractal dimension over a range of 10 to 10^5 years (Fluegeman & Snow 1989).

Considering the global distribution of the core locations, the variety of water masses and the different foraminifera species used for measuring the isotopic values, it is remarkable that the fractal dimensions estimated for the $\delta^{18}O$ records for time scales < 20 ka fall into a fairly narrow range. We interpret this as an expression of the dominance of the global ice-volume signal over the regional signal (water temperature, habitat). This is in accordance with our observation that the fractal dimension (for the same time scale using, the method described above) obtained from the SPECMAP stack (Imbrie et al. 1984), which can be assumed as ice-volume proxy, is $D = 1.48 \pm 0.01$ and, thus, coincides with our average fractal dimension for the τ_S group.

From the observation that the lowest fractal dimensions in the τ_S group stem from deep-water records, one may hypothesize that this is caused by the slower response of the deep ocean compared to the surface-water masses. Similarly one may argue that the high fractal dimension obtained from the high latitude surface record (ODP 643) is due to the proximity of this site to the location of ice formation. However, the average present-day deep-ocean mixing time is on the order of 1 ka, and surface water mixes in a few decades (e.g. Murray 1992). Since these time scales are shorter than the minimum time scale in our investigation, even the deep ocean can be assumed to be well mixed, thus refuting the above implications. Since the southern hemisphere high latitude surface-water record (DSDP 594) does not show a similar high fractal dimension, we regard the high fractal dimension estimated for core ODP 643 as an outlier. The inference about deep-water masses is also invalidated by the fact that different fractal dimensions arise from cores that document the same water mass (ODP 607/658: North Atlantic deep water; ODP 677/RC 13-110: Pacific deep water). We attribute these differences either to sampling errors, which are higher than those being assumed, or to errors in the core stratigraphy.

Looking at the fractal dimensions for time scales longer than ~20 ka, the finding that $D_l > D_S$ is somewhat curious. In terms of a fractional Brownian function this could be interpreted as a trend towards higher antipersistence (Feder 1988) of the underlying physical system or, in terms of a spectral representation, towards a white-noise spectrum. However, this interpretation is unreasonable if one considers the underlying climate system. Especially the ocean should act as a low-pass filter and thus lead towards higher persistence, resulting in a red-noise spectrum. The additional observation that no evidence for self-affinity was found for time scales exceeding ~60 ka points to the possible effect that periodic components in the time series bias the estimated fractal dimension. A likely source of such periodic elements are the Milankovic´ frequencies [i.e. periodic variations of the Earth's orbit, which are well documented in the deep-sea sedimentary record (e.g. Imbrie et al. 1984)], particularly the two strongest components with main periods of 41 and 100 ka . So far we have not been able to discriminate whether the above observations are artifacts or whether they imply that over certain time scales no self-affinity exists.

Finally, the estimated fractal dimensions are, due to the goodness-of-fit test, a function of measurement uncertainties. Assuming larger errors would result in a significant fit of the model (Eq. 3) over a *larger range* of time scales (and at the same time the number of fractal dimensions necessary to describe the time series would decrease). Due to the shape of the model function this would result in higher fractal dimensions than those given.

Appendix

Fractal sets can be scaled according to power laws as in Equation 3. It is very common to determine the fractal dimension by the linearization of such power laws. Instead of fitting a nonlinear model to the data (which requires extensive numerical calculations), the data are transformed (i.e. by taking logarithms) in order to yield a linear regression problem (which is computationally easy to handle). However, estimating fractal dimensions from linearized data is only an approximate method, since linearizing transformations change the statistical distribution of the errors associated with data (Bard 1974, p. 79).

Assume the following power-law function:

$$\mu_i = f(x) = \beta_0 x_i^{\beta_1}$$

This nonlinear model can be linearized by means of a logarithmic transformation:

$$\ln \mu_i = \ln \beta_0 + \beta_1 \ln x_i \qquad \text{(A1)}$$

Let y_i be realizations of this function and ε an error term accounting for the noise in the data. The least-squares regression method assumes ε to be additive and Gaussian distributed, $N(0,\sigma)$. Hence, Equation A1 becomes:

$$\ln y_i = \ln \beta_0 + \beta_1 \ln x_i + \varepsilon$$

This means, however, that in terms of the original data the error becomes *multiplicative*:

$$y_i = \beta_0 x_i^{\beta_1} \cdot e^{\varepsilon} \quad \text{(A2)}$$

Since the assumption concerning the error term in Equation A2 does not hold true for the data used in this study, the linearization transformation may lead to significantly biased estimations of the parameters β_0 and β_1.

Comparison of fractal dimensions obtained by a linear regression in log-log space with those obtained by fitting a nonlinear model to the data points reveal differences on the order of 10%. Therefore, determinations of fractal dimensions should be done by the use of nonlinear models instead of simple, but inaccurate, linear models.

Acknowledgments. We thank J.H. Kruhl and an anonymous reviewer for their comments, which helped to improve the final manuscript. We are also grateful to M. Raymo and R. Tiedemann for providing us their $\delta^{18}O$ data. This work was supported by the *Deutsche Forschungsgemeinschaft*: grant TH 200/10-2 and *Graduiertenkolleg 'Dynamik globaler Kreisläufe im System Erde'*.

References

Bard Y (1974) Nonlinear parameter estimation. Academic Press, New York,

Clemens S, Prell W, Murray D, Shimmield G, Weedon G (1991) Forcing mechanisms of the Indian Ocean monsoon. Nature 353: 720-725.

deMenocal PB, Ruddiman WF, Pokras EM (1993) Influences of high- and low-latitude processes on African terrestrial climate: Pleistocene eolian records from equatorial Atlantic Ocean Drilling Program Site 663. Paleoceanogr 8: 209-242.

Feder J (1988) Fractals. Plenum Press, New York.

Fluegeman RH Jr, Snow RS (1989) Fractal analysis of long-range paleoclimatic data: Oxygen isotope record of Pacific core V28-239. PAGEOPH 131: 307-313.

Higuchi T (1988) Approach to an irregular time series on the basis of the fractal theory. Physica D 31: 277-283.

Imbrie J, Hays JD, Martinson DG, McIntyre A, Mix AC, Morley JJ, Pisias NG, Prell WL, Shackleton NJ (1984) The orbital theory of Pleistocene climate: support from a revised chronology of the marine $\delta^{18}O$ record. In: Berger A, Imbrie J, Hays J, Kukla G, Saltzman B (eds) Milankovitch and climate, vol Part I. Reidel, Dordrecht, pp 269-305.

Mandelbrot BB (1967) How long is the coast of Britain? Science 155: 636-638.

Mandelbrot BB (1977) Form, chance, and dimension: fractals. Freeman, San Francisco.

Mix AC (1992) The marine oxygen isotope record: Constraints on timing and extent of ice-growth events (120-65 ka). In: Clark PU, Lea PD (eds) The last interglacial-glacial transition in North America. Geol Soc Amer Spec Paper 270, pp 19-30.

Mix AC, Pisias NG, Zahn R, Rugh W, Lopez C, Nelson K (1991) Carbon 13 in Pacific deep and intermediate waters, 0-370 ka: implications for ocean circulation and Pleistocene CO_2. Paleoceanogr 6: 205-226.

Murray JW (1992) The oceans. In: Butcher SS, Charlson RJ, Orians GH, Wolfe GV (eds) Global biogeochemical cycles, International Geophysics Series 50. Academic Press, London, pp 175-211.

Nelson CS, Hendy CH, Cuthbertson AM, Jarrett GR (1986) Late Quaternary carbonate and isotope stratigraphy, subantarctic Site 594, southwest Pacific. In: Kennett JP, von der Borch CC, et al. (eds) Init. Repts. DSDP Leg 90. Washington, U.S. Govt. Printing Office, pp 1425-1436.

Press WH, Flannery BP, Teukolsky SA, Vetterling WT (1989) Numerical recipes in Pascal. Cambridge Univ Press, Cambridge.

Ruddiman WF, Raymo M, McIntyre A (1986) Matuyama 41,000-year cycles: North Atlantic Ocean and northern hemisphere ice-sheets. Earth Planet Sci Lett 80: 117-129.

Ruddiman WF, Raymo M, Martinson, DG, Clement, BM, Backman, J (1989) Pleistocene evolution: northern hemisphere ice sheets and north Atlantic circulation. Paleoceanogr 4: 353-412.

Shackleton NJ, Hall MA (1989) Stable isotope history of the Pleistocene at ODP Site 677. In: Becker K, Sakai H, et al. (eds) Proc. ODP, Sci Results 111. College Station, TX (Ocean Drilling Program), pp 295-316.

Shackleton NJ, Berger A, Peltier WR (1990) An alternative astronomical calibration of the lower Pleistocene timescale based on ODP Site 677. Trans R Soc Edinburgh: Earth Sci 81: 251-261.

Tiedemann R (1991) Acht Millionen Jahre Klimageschichte von Nordwest Afrika und Paläo-Ozeanographie des angrenzenden Atlantiks: Hochauflösende Zeitreihen von ODP-Sites 658-661. Ber Geol-Paläont Inst Univ Kiel 46: 1-190

Turcotte DL (1992) Fractals and chaos in geology and geophysics. Cambridge Univ Press, Cambridge.

Wolf TCW (1991) Paläo-ozeanographisch-klimatische Entwicklung des nördlichen Nordatlantiks seit dem späten Neogen (ODP Legs 105 und 104, DSDP Leg 81). Geomar Rep 5: 1-92.